2011

Ontogenetic Changes in the Bell Morphology and Kinematics and Swimming Behavior of Rowing Medusae: the Special Case of the Limnomedusa Liriope tetraphylla

Tasia Blough
Roger Williams University

Sean Colin
Roger Williams University, scolin@rwu.edu

John H. Costello
Providence College

Antonio C. Marques
University of Sa˜o Paulo

Recommended Citation

Blough, T., Colin, S. P., Costello, J. H., Marques, A. C. 2011. Ontogentic changes in the bell morphology and kinematics and swimming behavior of rowing medusae: the special case of the limnomedusa Liriope tetraphylla. *Biological Bulletin*. 220: 6-14.

Reference: *Biol. Bull.* **220:** 6–14. (February 2011)

Ontogenetic Changes in the Bell Morphology and Kinematics and Swimming Behavior of Rowing Medusae: the Special Case of the Limnomedusa *Liriope tetraphylla*

TASIA BLOUGH[1], SEAN P. COLIN[1,*], JOHN H. COSTELLO[2], AND ANTONIO C. MARQUES[3]

[1]*Environmental Sciences and Marine Biology, Roger Williams University, Bristol, Rhode Island 02809;* [2]*Biology Department, Providence College, Providence, Rhode Island 02918; and* [3]*Department of Zoology, Institute of Biosciences, University of São Paulo, São Paulo, Brazil*

Abstract. Swimming animals may experience significant changes in the Reynolds number (*Re*) of their surrounding fluid flows throughout ontogeny. Many medusae experience *Re* environments with significant viscous forces as small juveniles but inertially dominated *Re* environments as adults. These different environments may affect their propulsive strategies. In particular, rowing, a propulsive strategy with ecological advantages for large adults, may be constrained by viscosity for small juvenile medusae. We examined changes in the bell morphology and swimming kinematics of the limnomedusa *Liriope tetraphylla* at different stages of development. *L. tetraphylla* maintained an oblate bell (fineness ratio $\approx$ 0.5–0.6), large velar aperture ratio ($R_v \approx$ 0.5–0.8), and rapid bell kinematics throughout development. These traits enabled it to use rowing propulsion at all stages except the very smallest sizes observed (diameter = 0.14 cm). During the juvenile stage, very rapid bell kinematics served to increase *Re* sufficiently for rowing propulsion. Other taxa that use rowing propulsion as adults, such as leptomedusae and scyphomedusae, typically utilize different propulsive strategies as small juveniles to function in low *Re* environments. We compared the performance values of the different propulsive modes observed among juvenile medusae.

Introduction

Swimming animals use body motions to manipulate their surrounding fluids and create the thrust necessary for propulsion. Propulsive modes can be characterized by analyzing the flow patterns generated in the wake of swimming animals. For medusae, wake structures have been used to categorize their propulsion as either jetting or rowing (Colin and Costello, 2002; Dabiri *et al.*, 2005, 2006). The relevance of these two propulsive modes extends beyond merely swimming behavior because swimming modes relate directly to morphological and foraging characteristics of medusae (Colin and Costello, 2002; Colin *et al.*, 2003; Costello *et al.*, 2008).

Jetting medusae generally possess small, prolate bells (*i.e.,* high aspect or fineness ratio) with constricted orifices leading to their subumbrellar cavities (Colin and Costello, 2002; Dabiri *et al.*, 2006). Swimming by a jetting medusa is characterized by rapid, full-body bell contractions that force a stream of fluid out of the subumbrellar cavity, jetting the medusa forward (Daniel, 1983; Colin and Costello, 2002). During this process, a starting vortex is formed that quickly moves downstream, away from the medusa, leaving a wake of moderately spaced vortices (Dabiri *et al.*, 2006). Jet-propelled medusae reach high velocities and are thus highly proficient swimmers, but this propulsive strategy is energetically inefficient compared to other modes (Daniel, 1985; Sahin *et al.*, 2009; Dabiri *et al.*, 2010). However, the energetic costs associated with swimming by jetting may be tolerable since jetting medusae generally only swim with short bursts to reposition themselves in the water column or escape predation. Consequently, these medusae spend a majority of their time resting motionlessly while foraging as ambush predators (Colin and Costello, 2002; Colin *et al.*, 2003).

Received 29 September 2010; accepted 14 December 2010.
* To whom correspondence should be addressed. E-mail: scolin@rwu.edu

In contrast, rowing medusae usually possess oblate bells (*i.e.,* low fineness ratio) with large subumbrellar orifices. These features are conducive to a rowing propulsion that is characterized by slower, non-uniform bell contractions to generate forward thrust (Colin and Costello, 2002; Weston *et al.*, 2009). During the expansion and contraction phases of the swimming cycle, bell motion creates a set of interacting vortices. As the bell expands, a "stopping vortex" is formed on the interior of the bell. Immediately after stopping vortex formation, a contraction of the bell generates a "starting vortex" along the bell margin. The stopping vortex, moving in the opposite direction relative to the starting vortex, interacts with and slows the spinning of the starting vortex as the medusa is propelled forward (Dabiri *et al.*, 2005). The resultant vortex complex relies on inertial forces and inhibits the downstream movement of the vortices (Dabiri *et al.*, 2005). The net impact of this vortex interaction is a slower, but more efficient, mode of swimming (Sahin *et al.*, 2009; Dabiri *et al.*, 2010). A related consequence of a rowing propulsive mode is the circulation of large water volumes through the bell and tentacles (Dabiri *et al.*, 2005). These circulation patterns serve to entrain prey and generate high prey encounter rates. Because this propulsive strategy minimizes energy input (Sahin *et al.*, 2009; Dabiri *et al.*, 2010) while maximizing prey encounters, rowing species generally swim continuously and forage using a feeding current (Colin and Costello, 2002; Colin *et al.*, 2003; Kiørboe, 2010).

Propulsive strategies available to medusae appear to be constrained by size. Propulsive models indicate that jet-based propulsion by medusae is limited to bell diameters below about 10 cm (Dabiri *et al.*, 2007; Costello *et al.*, 2008). In contrast, rowing does not appear to have upper size constraints and has been observed in medusae of all bell sizes (Dabiri *et al.*, 2007; Costello *et al.*, 2008). Lower size constraints have not been observed for either medusan propulsive mode (Weston *et al.*, 2009); however, Cantwell (1986) calculated that jet vortices do not form below a Reynolds number (*Re*) of 6. This lower *Re* limit may constrain jet propulsion at the smallest sizes. In contrast, rowing propulsion requires an interaction between the starting and stopping vortices which requires higher levels of inertia in the wake (Dabiri *et al.*, 2005; Weston *et al.*, 2009). Consequently, medusae must theoretically create water flow with *Re* exceeding 6 for successful rowing. Although most medusae generate *Re* greatly exceeding this level (Gladfelter, 1973), it is possible that small medusae may have difficulty producing high-velocity fluid reaching *Re* necessary for the vortex interactions that characterize rowing propulsion.

The fluid environment of newly budded medusae (often of bell diameter as small as 1 mm) is considerably different from that of adult medusae because viscous forces are equally as important as inertial forces (Higgins *et al.*, 2008; Feitl *et al.*, 2009). Consequently, propulsive mechanisms described for rowing adults, which largely rely upon inertial forces (Dabiri *et al.*, 2005), may not apply to juvenile medusae. So how then do these tiny medusae deal with these transitions in fluid environments? Weston *et al.* (2009) studied this question for two leptomedusan species, *Aequorea victoria* and *Eutonina indicans,* and found that these medusae undergo a number of morphological and behavioral transformations to adjust for changes in their fluid environments. Similar observations have been made for scyphomedusae that develop from ephyrae, characterized by bells with large clefts separating lappets, into adults with continuous bell morphologies (Higgins *et al.*, 2008; Feitl *et al.*, 2009).

In this study we examine the propulsion of *Liriope tetraphylla* (Chamisso and Eysenhardt, 1821) throughout its development. *L. tetraphylla*, formerly assigned to the trachymedusan family Geryoniidae, appears to be better assigned as a limnomedusan in the family Olindiasidae (Collins *et al.*, 2008; Collins, 2009). Like leptomedusae, *L. tetraphylla* is initally very small ($\approx$1 mm), but unlike leptomedusae, it apparently does not undergo a dramatic change in bell morphology during development. Therefore, to examine how the fluid interactions and propulsion of *L. tetraphylla* change throughout development, we quantified the bell morphology, swimming kinematics, and fluid interactions of the swimming limnomedusa at different stages of development.

Materials and Methods

Specimen collection and microvideography

Individual medusae of *Liriope tetraphylla* were collected by hand from surface waters adjacent to the Centro de Biologia Marinha (CEBIMar-USP), Universidade de São Paulo, São Sebastião, Brazil. Medusae were immediately transported to the laboratory and kept in tanks at room temperature (20 °C) filled with filtered seawater. Individuals were used within 36 h of collection.

The swimming kinematics and fluid flow were visualized by placing medusae in variably sized rectangular glass containers that were $>$10 body-lengths wide and were side-illuminated using halogen lights. To visualize and record bell and swimming kinematics, freely swimming individuals were recorded at 250 frames per second (fps) and swimming sequences transferred to miniDV videotape. Flow around the medusae was visualized qualitatively with fluorescein dye and quantitatively by tracking natural particles and *Artemia* sp. cysts (Dabiri *et al.*, 2005; Weston *et al.*, 2009). To minimize error in the z-dimension, we analyzed only swimming profiles in which the individuals remained within focus for the entire sequence.

Morphological traits of medusae

Changes in bell morphology during development were quantified by measuring the fineness ratio, F, and velar aperture ratio, R_v, of different sized medusae when they were in a fully expanded, relaxed state (Weston *et al.*, 2009). Fineness was calculated as

$$F = \frac{h}{d}$$

where h is bell height and d is bell diameter. Instantaneous fineness ratio, F_i, denotes the fineness ratio of medusae at a given point in the swimming cycle and is used to compare variations in changes of bell shape throughout pulsations of different medusae. F_i is generally highest at the point of full contraction and lowest at maximum relaxation. The velar aperture area ratio (R_v) is the ratio of the area of the subumbrellar orifice, or velar aperture, over the area of the velum at relaxation. This reduces to

$$R_v = \frac{v^2}{d^2}$$

where v is the orifice diameter. The higher the velar aperture ratio the larger the orifice opening is relative to the bell diameter.

Kinematic analysis of swimming

To collect kinematic data, individuals were tracked during swimming bouts that consisted of three to six bell pulsation cycles within a single focal plane. Swimming segments were videotaped at an angle perpendicular to the plane so that a side profile of medusae swimming vertically was used for measurements. From the bell kinematics we measured velocity (u), Reynolds number (Re), contraction time of the bell (time between start of contraction and full contraction), and time between pulses (amount of time maximum expansion is sustained between pulses). Three points on the medusae (bell apex and the two outermost tips of the bell margin) were tracked at 0.004 s (t) intervals through time using Maxtraq motion analysis software, ver. 2.2.1.1. Instantaneous values are signified by the subscript i.

Distance traveled (D) between intervals was calculated as

$$D_i = \sqrt{(x_{t+1} - x_t)^2 + (y_{t+1} - y_t)^2}.$$

The velocity (u) was calculated as an average over two frames or time intervals (t):

$$u_i = \frac{D_t + D_{t-1}}{2t}.$$

Maximum velocity (u_{max}) for each medusa was calculated as an average of the maximum velocities reached over consecutive pulses as

$$u_{max} = \frac{u_1 + u_2 + u_3}{P},$$

Where P is the number of pulses used in the average.

Reynolds number (Re) was calculated as

$$Re_i = \frac{d_i u_i}{v},$$

where d_i and u_i are the instantaneous medusan diameter and velocity, respectively, and n is the kinematic viscosity of seawater.

Figures plotting kinematic data and data based on kinematic measurements (*e.g., Re*) *versus* bell diameter display the mean (±s.d.) of the kinematics over three consecutive pulsation cycles for each individual. Means were used to reduce the overall variability, and error bars (±s.d.) are presented to provide information on the variability of these traits within each individual. However, since these values are not true replicates, only the means were used for the regression analysis (standard regression using SigmaStat Software, ver. 3.5) to compare kinematic traits among individuals.

Fluid flow interpretation

Understanding fluid flow structures produced by medusae is essential to interpreting modes of propulsion used by *L. tetraphylla*. Flow visualizations using fluorescein dye enabled us to examine vortex spacing and dynamics. The interactions of starting and stopping vortices, a phenomenon that is essential to rowing propulsion, inhibit the momentum of the total vortex complex and can thus be measured by the speed that the trailing vortices travel away from the medusa (Dabiri *et al.*, 2005). The velocities of vortices were quantified at the end of a contraction, using the distance between the core of the ring and the posterior end of the medusa divided by the contraction time (Weston *et al.*, 2009).

Stopping vortices are initially produced inside the bells of rowing medusae and then ejected out of the bell with a starting vortex. We used particle-tracking footage to determine the Reynolds numbers ($Re_{stopping}$) of such stopping vortices throughout various sizes of medusae to determine how significant a role the stopping vortices played in the propulsion of each medusa. To measure Re inside the bell cavity (see Fig. 4), $d_{stopping}$ was determined from the distance between the inner surface of the exumbrella and the manubrium. This is the space in which the stopping vortex rotates. The velocity, $u_{stopping}$, was measured from particles entering the bell and circulating in the stopping vortex during bell expansion. We were unable to measure the distance particles traveled from frame to frame because the sequences were not captured at a high enough frame rate; consequently, many particles appeared as streaks. We instead used the length of the streaks and divided them by the

frame rate to determine the velocity of each particle. This measurement required particles to be entering the bell during the onset of bell expansion; unfortunately, this was only observed for four medusae, limiting our sample size.

Results

Bell morphology

The bell aspect ratio (Fig. 1A) and orifice size (Fig. 1B) of *Liriope tetraphylla* did not change appreciably through development. Some trends were observed but were statistically weak (Fig. 1). Compared to the morphological changes seen during the development of Leptomedusae (Weston *et al.*, 2009), those of *L. tetraphylla* were minor.

Bell kinematics

Contraction duration (*i.e.,* time it took the bell to contract) increased linearly with bell diameter (Fig. 1C). In addition, the time between pulses decreased as bell diameter increased. The two smallest medusae analyzed (<0.2 cm diameter) paused briefly between pulses; but by 0.2 cm in diameter only an instantaneous pause, which remained constant through development, was observed between pulses (Fig. 1D). The total pulse times of medusa swimming profiles were very consistent at 0.1 ± 0.01 s.

To put these pauses into perspective, the pauses of the smallest medusae were about twice as long as those of larger medusae, but they still lasted only about 0.03 s. When compared to the durations of the full pulse cycles, which are approximately 0.1 s, these pauses were ≈25% of the duration of the cycles. Profiles of fineness ratio (F_i) over time of a small (0.17 cm diam.) and a large (0.5 cm diam.) medusa illustrate these kinematic differences (Fig. 2 left and right columns, respectively). In essence, the swimming cycles of medusae at the earliest stages can be described as quick, short pulses followed by brief pauses, whereas the cycles of mature medusae were continuous.

Fluid interactions

A comparison of maximum Reynold's numbers (Re_{max}) throughout development showed that Re_{max} increased by more than an order of magnitude as the medusae grew (Fig. 3A). For the smallest medusae, Re_{max} peaked at ≈10, while for the largest it peaked at ≈180. Consequently, they undergo a transition in the fluid environment where inertial forces become more important. The effects of the different fluid environments on the swimming kinematics can be seen by comparing the position and swimming velocity throughout the swimming cycles (Fig. 2). Owing to the small Re_{max}, the small medusae moved backward during the bell relaxation phase of the swim cycle (Fig. 2B and C) while the momentum of the larger medusae enabled them to continually glide forward with a positive velocity throughout the swim cycle (Fig. 2F and G). Interestingly, small medusae experienced a brief interval of forward motion during the pause after full bell relaxation. This was not due to advection in the vessels, and it occurred while the stopping vortex inside the bell was still rotating. Consequently, it appears

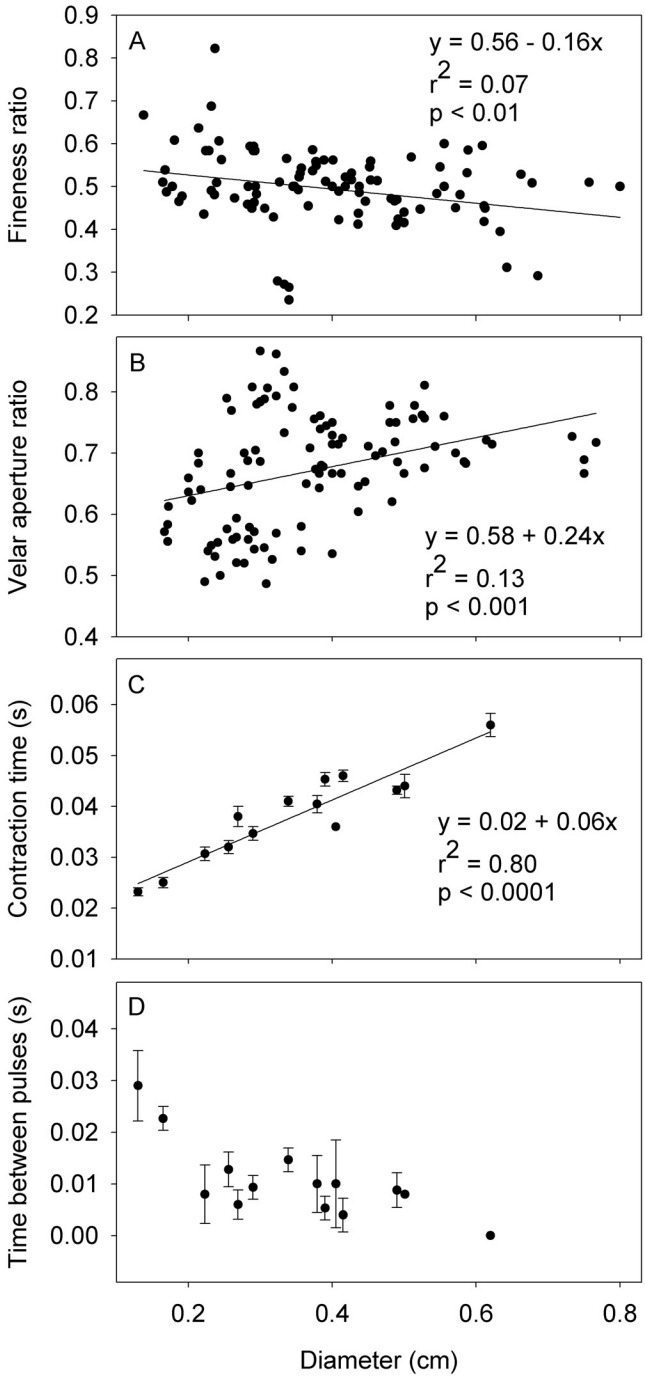

Figure 1. Changes in bell morphology (A, B) and swimming kinematics (C, D) of *Liriope tetraphylla* as a function of bell diameter. Kinematic data points (C and D) represent an average (±s.d.) obtained over 3 to 6 consecutive pulsations by an individual swimming medusa.

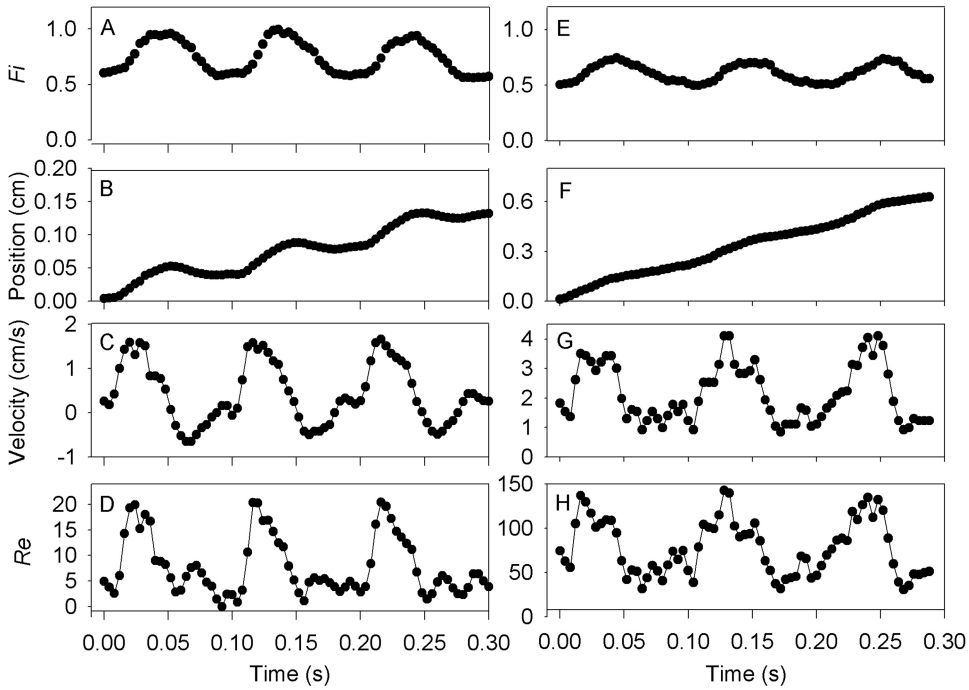

Figure 2. Representative kinematic profiles of a small (0.18 cm; A–D) and a large (0.49 cm; E–H) medusa over three consecutive propulsive cycles. Note that while the scales of *x*-axes, representing time, are the same for both medusae, the scales of *y*-axes vary.

that the rotation of the stopping vortex within the subumbrellar cavity provided a low amount of forward thrust. This is consistent with computational studies on rowing propulsion in larger individuals (Sahin *et al.*, 2009).

The influence of the alteration of *Re* environments accompanying medusan development was also evident in wake dynamics of different size medusae. The rotation velocities observed in the starting and stopping vortices decreased with decreasing medusan size. Estimates of the $Re_{stopping}$ inside the bell during bell expansion ranged from ≈64–128 and increased with bell diameter (Fig. 4). Extrapolating this relationship to smaller sizes suggests that the $Re_{stopping}$ would be too small for vortex formation ($Re < 6$; Cantwell, 1986) for medusae smaller than 0.14 cm diameter (Fig. 4). Unfortunately, we did not have video sequences with particles entering the bell to measure $Re_{stopping}$ at these small sizes. However, we observed that rotation of dye within the subumbrellar cavity ceased as soon as bells of medusae less than 0.14 cm bell diameter stopped expanding. For medusae above that size threshold, we observed rotation of the stopping vortex after bell expansion was complete. This rotation increased with diameter and resulted in greater stopping vortex circulation. In turn, greater stopping vortex dimensions resulted in more pronounced interactions between stopping and starting vortices as bell diameter increased during medusan development. The downstream movement of a vortex complex was used to measure the strength of stopping-starting vortex interactions (Weston *et*

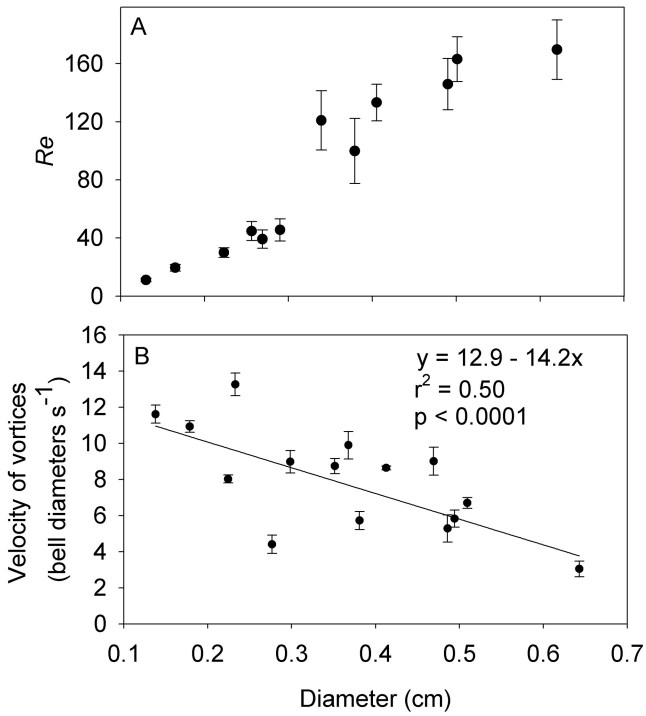

Figure 3. Relationship between (A) Re_{max} and (B) the velocity of trailing vortex rings as they travel downstream away from medusae of various sizes. Each data point represents the average (±s.d.) of 4 to 7 pulsation cycles of an individual medusa.

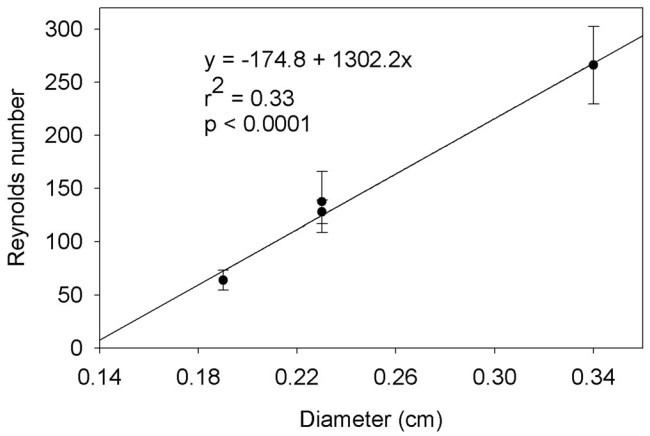

Figure 4. Reynolds number (*Re*) of fluid entering the bells of different-sized *Liriope tetraphylla* during bell expansion. Trend line represents the linear regression of the $Re_{stopping}$ *versus* size. Note that the *y*-intercept at 0.14 cm is $Re = 6$, which is the minimum *Re* at which jet vortex rings form (Cantwell, 1986). The points represent different medusae, and the error bars (±s.d.) were calculated by tracking multiple particles (2–4) within a medusa.

al., 2009), and the velocity at which a vortex complex moved away from a medusa decreased as the medusa's bell diameter increased (Fig. 3B).

Swimming kinematics

The maximum swimming velocities of *L. tetraphylla* initially increased with bell diameter. However, swimming velocities plateaued after medusae reached a diameter of 0.3 cm (Fig. 5). As noted, small medusae lacked forward momentum and exhibited negative velocities during bell expansion (Fig. 2C and E). This was observed for all medusae less than 0.3 cm in diameter, but was not observed for any medusae above this diameter.

Discussion

Many aquatic organisms experience significant changes in the Reynolds number (*Re*) of their fluid environment as they grow and develop. Often morphological and behavioral changes observed during development are evolved solutions that enable these organisms to function efficiently—for example, swim—in these changing environments (Batty, 1984; Williams, 1994; Feitl *et al.*, 2009; Nawroth *et al.*, 2010). Medusae are examples of aquatic organisms that experience large changes in *Re* as they grow, transitioning from flow regimes characterized by $Re < 10$, where viscous forces are important, to regimes characterized by $Re > 100$, where inertial forces dominate (Fig. 3; Higgins *et al.*, 2008; Weston *et al.*, 2009). Throughout these transitions, medusae must continue to manipulate their surrounding fluids in order to move, feed, and reproduce. The solutions to these challenges vary among medusan taxa (Nawroth *et al.*, 2010).

Judging from the current work and previous studies (Higgins *et al.*, 2008; Feitl *et al.*, 2009; Weston *et al.*, 2009), rowing medusae that develop through intermediate *Re* environments appear to have converged upon three propulsive strategies of early development. One strategy, observed among leptomedusae and anthomedusae, is to swim *via* jet propulsion as juveniles (Weston *et al.*, 2009). A second strategy, observed among scyphomedusae and the small hydromedusa *Obelia* spp., is to swim using drag-based paddling (Feitl *et al.*, 2009). Both these strategies characterize taxa that swim using rowing propulsion as adults—for example, leptomedusae (Weston *et al.*, 2009) and scyphomedusae (Higgins *et al.*, 2008). Consequently, morphological and behavioral modifications occur during development to accommodate these propulsive changes. In this study, we found that the rowing limnomedusa *Liriope tetraphylla* did not conform to either of these two strategies. Instead, *L. tetraphylla* employs a third strategy involving morphological and swimming traits associated with rowing propulsion throughout development. Only at the very smallest sizes (<0.3 mm diameter), when viscous forces constrained the wake dynamics required for rowing propulsion (*i.e.,* starting-stopping vortex interaction) did its wake resemble that of jet propulsion (*i.e.,* no interaction between stopping and starting vortices).

The morphological and kinematic requirements of jet propulsion and drag-based paddling differ from those required for rowing propulsion. Consequently, morphological and kinematic modifications observed throughout the development of medusan taxa depend largely upon their juvenile propulsive strategy (Costello *et al.*, 2008; Higgins *et al.*, 2008; Weston *et al.*, 2009; Feitl *et al.*, 2009). The thrust generated using jet propulsion is determined by the momentum flux of fluid from the subumbrellar cavity during bell

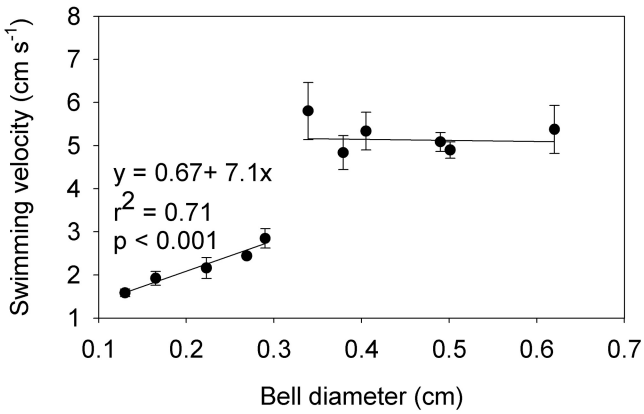

Figure 5. Peak swimming velocity in propulsive cycles of developing *Liriope tetraphylla*. Each data point is an average (±s.d.) obtained over 3 to 6 consecutive pulsations by an individual swimming medusa.

Table 1

Comparison of bell morphology and kinematics and swimming performance of different medusan taxa that use different propulsive strategies as juveniles than their rowing adult forms

Class	Hydrozoa	Hydrozoa	Scyphozoa
Order	Leptomedusae	Limnomedusae	Semaeostomeae
Genus	*Aequorea*[1]	*Liriope*[2]	*Cyanea*[3]
Juvenile			
Propulsive mode	**Jetting**	**Rowing**	**Paddling**
Size (cm)	0.1	0.2	0.2
Maximum velocity (cm s^{-1})	2.8	1.6	0.7
Max. Reynolds number (*Re*)	24	20	8
Fineness ratio	3.0	0.6	0.3
Aperture velar ratio	0.1	0.6	na
Contraction time (s)	0.1	0.02	0.1
Adult			
Propulsive mode	**Rowing**	**Rowing**	**Rowing**
Size (cm)	2.9	0.6	2.6
Maximum velocity (cm s^{-1})	1.3	6.0	5.0
Max. Reynolds number (*Re*)	328	303	1023
Fineness ratio	0.6	0.5	0.3
Aperture velar ratio	0.8	0.7	na
Contraction time (s)	0.3	0.05	0.5

[1] Data from Weston *et al.* (2009).
[2] Data from this study.
[3] Data from Higgins *et al.* (2008).

contraction and is maximized by a rapid bell contraction and fluid ejection through a small orifice. Accordingly, leptomedusae, such as *Mitrocoma cellularia*, *Aequorea victoria,* and *Eutonina indicans,* that use jet propulsion during early developmental stages have prolate bells with narrow orifices (*i.e.,* low aperture velar ratios) and short contraction times during these early stages (Table 1; Fig. 6A Jet). The transition into rowing adults entails rapid maturation of oblate bells with high velar aperture ratios and slower bell contractions (Table 1; Fig. 6B; Widmer, 2004; Weston *et al.*, 2009). Alternatively, medusan juveniles using drag-based paddling, a common low *Re* mode of propulsion used by some cilia (Vogel, 1994; Biewener, 2003) and the limbs of crustaceans (Williams, 1994), insects (Blake, 1986), and small vertebrates (Blake, 1981), have completely different morphological and kinematic requirements. As the name suggests, thrust is produced by the force of drag acting on the "paddle" (the bell margin or ephyral lappet), and net forward thrust is produced as long as the drag acting on the paddle during the power stroke is greater than during the recovery (Vogel, 1994; Biewener, 2003). Thrust during each phase of the stroke is directly related to the projected surface area, velocity, and stroke length (*i.e.,* amplitude) of the paddle (Williams, 1994). The bell kinematics of juvenile medusae that use this mode reflect these needs. During relaxation, the bells of scyphozoan ephyrae are inverted (Fig. 6A Paddling; Feitl *et al.*, 2009). As a result, the amplitude of the stroke is greater and the bell moves normal to flow for a longer distance than occurs with adult bell morphology and kinematics. In addition, since paddling does not rely on jet ejection from a bell volume but only on the drag acting on the paddle surface, ephyrae are able to exploit discontinuous bells (termed lappets) that use less tissue but produce sufficient thrust (Feitl *et al.*, 2009; Nawroth *et al.*, 2010). The tentacles of *Obelia* spp. also probably serve a similar function (unpubl. data, Costello *et al.*, 2008). These modest alterations in morphology and kinematics interact sufficiently differently with the surrounding fluid to alter the type of propulsion—that is, thrust generation by the bell.

The morphological and kinematic changes observed during the development of *L. tetraphylla* are minor in comparison to those of leptomedusae and scyphomedusae. Hence, the bell morphology of *L. tetraphylla* medusae, characterized by low fineness ratio and low aperture velar ratio, did not change appreciably during development and was sufficiently oblate to form stopping vortices during bell expansion (Fig. 6A Rowing). Medusae above 0.2 cm bell diameter were characterized by bell contractions that generated flows inside the bell with sufficient momentum (Fig. 4) to enable stopping vortices to continue rotating into the next swim cycle. These stopping vortices interacted with the starting vortices formed during subsequent pulses. Such vortex interactions inhibit downstream velocities of the vortex complex (Fig. 3b), while also increasing the total fluid volume entrained into the wake. Wake vortex volume is directly related to thrust production, and the greater wake vortex volume produced by the stopping-starting vortice interac-

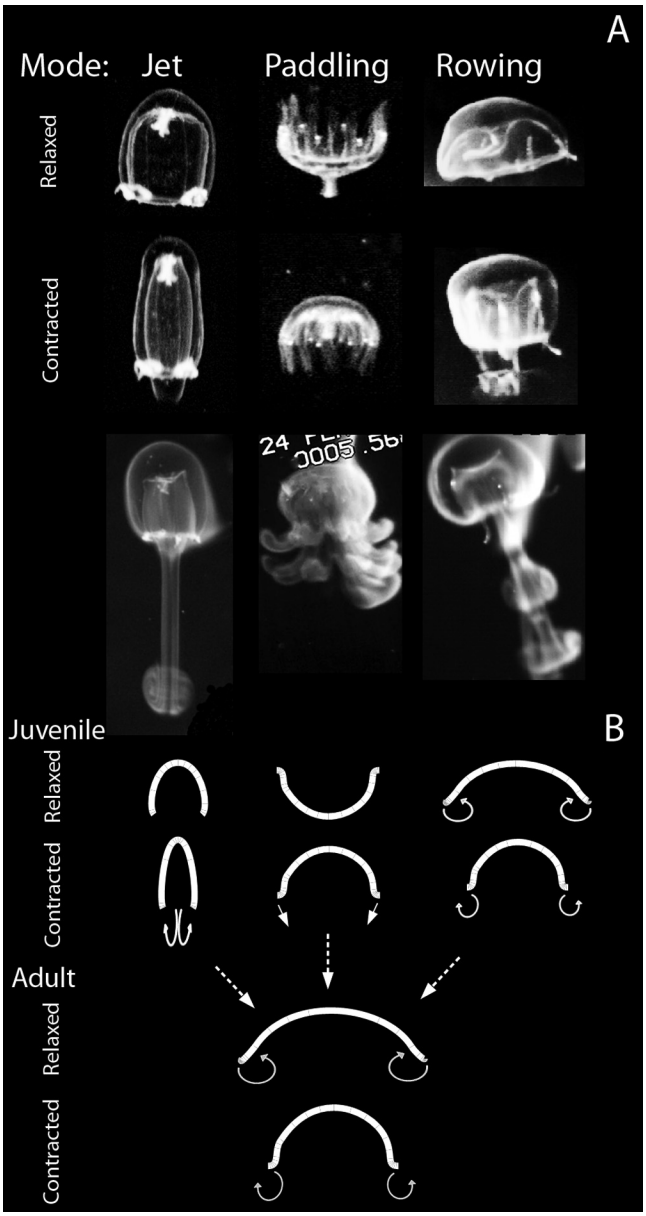

Figure 6. (A) Images of jetting (*Aequorea victoria*, 1 mm relaxed diameter), drag-based paddling (*Cyanea capillata*, 2 mm diameter), and rowing (*Liriope tetraphylla*, 1.3 mm diameter) juvenile medusae and the wake they produce (visualized using fluorescein dye). Notice the long jet *versus* the closely spaced vortices for the jetting and rowing medusae, respectively. (B) A schematic of the bell morphology, kinematics, and prominent wake features (narrower arrows) of the three modes of propulsion observed among juvenile medusae that use rowing propulsion as adults. The jetting medusae produce a starting vortex, the rowing produces stopping (as bell relaxes) and starting (as bell contracts) vortices, and drag-based paddling medusae do not form full vortices during early stages.

tion increases the thrust generated by the medusae (Dabiri *et al.*, 2005). The swimming proficiency of *L. tetraphylla* increased greatly when it was large enough for stopping and starting vortices to interact (about 0.3 cm), and the swimming speed of *L. tetraphylla* peaked at this size.

The rowing mechanism of propulsion was not possible below 0.2 cm bell diameter, and these smallest medusae probably rely solely on a jet mechanism of propulsion. At this size, estimates of *Re* of the fluid inside the bell were below the *Re* threshold for the formation of vortex rings ($Re < 6$; Cantwell, 1986). Consequently, stopping vortex formation inside the subumbrella was inhibited and only the starting vortex, characteristic of jet propulsion, was available for thrust production. However, jet propulsion did not enhance the performance of these smallest individuals of *L. tetraphylla*. Because jet thrust depends upon high-velocity flow through a narrow aperture, the wide velar apertures and oblate bells of *L. tetraphylla* are minimally effective for generation of high jet thrust for swimming. Based on the kinematic model by Daniel (1983) where instantaneous thrust (T) equals $(\rho/Av)(dV_{si}/dt)^2$ [ρ = density of seawater, Av = orifice area, and dV_{si}/dt is the instantaneous change in subumbrellar volume over the change in time], we can estimate the thrust produced during contraction of *L. tetraphylla versus* a juvenile of *A. victoria* (representing a medusa whose morphology conforms to more optimal jetting characteristics; from Weston *et al.*, 2009) of the same size (0.15 cm diameter) to examine how oblate *versus* prolate morphologies and orifice size affect jet thrust. *L. tetraphylla* was able to produce a maximum thrust of only 0.074×10^{-5} *N* (mean [based on total contraction time and volume at the start and end of the contraction] = 0.038×10^{-5} *N*), while *A. victoria* produced a maximum of 0.56×10^{-5} *N* (mean = 0.24×10^{-5} *N*). Although *L. tetraphylla* juveniles contract almost 10 times more rapidly than juvenile leptomedusae, their oblate bells and large orifices are too large to form effective jets (Fig. 6). Consequently, *L. tetraphylla* juveniles swam more slowly than juvenile leptomedusa (Table 1).

Why have rowing medusae developed different propulsive strategies during the early developmental stages? Our comparative approach to swimming performance suggests that jetting outperforms both paddling and rowing at the smallest medusan sizes. Hence, we might expect jetting to confer some selective advantage at small sizes. However, swimming performance may not be a dominant trait under selective pressure during evolution of early life stages among medusan lineages, and considerations such as phylogenetic constraints (*e.g.,* Costello *et al.,* 2008) also complicate comparisons of developmental strategies. Although the rowing approach employed by *L. tetraphylla* appears to be a relatively uncommon solution to early medusan development, the wide distribution of *L. tetraphylla* throughout the world's oceans indicates the evolutionary success of this developmental pattern.

Acknowledgments

We thank Alvaro Migotto for his generous hospitality and use of the facilities at the Centro de Biologia Marinha (CEBIMar-USP), Universidade de São Paulo, São Sebastião, Brazil. We also appreciated the help of Lucilia Miranda. This work was funded by the National Science Foundation (grant numbers OCE-0350834 and OCE-0623508 to JHC; OCE-0351398 and OCE-0623534 to SPC.) and the Office of Naval Research (ONR N000140810654).

Literature Cited

Batty, R. S. 1984. Development of swimming movements and musculature of larval herring (*Clupea harengus*). *J. Exp. Biol.* **110:** 217–229.

Biewener, A. A. 2003. *Animal Locomotion*. Oxford University Press, Oxford.

Blake, R. W. 1981. Mechanics of drag-based mechanisms of propulsion in aquatic vertebrates. *Symp. Zool. Soc. Lond.* **48:** 29–53.

Blake, R. W. 1986. Hydrodynamics of swimming in the water boatman, *Cenocorixa bifida*. *Can. J. Zool*. **64:** 1606–1613.

Cantwell, B. J. 1986. Viscous starting jets. *J. Fluid Mech.* **173:** 159–189.

Colin, S. P., and J. H. Costello. 2002. Morphology, swimming performance, and propulsive mode of six co-occurring hydromedusae. *J. Exp. Biol.* **205:** 427–437.

Colin, S. P., J. H. Costello, and E. Klos. 2003. In situ swimming and feeding behavior of eight co-occurring hydromedusae. *Mar. Ecol. Prog. Ser.* **253:** 305–309.

Collins, A. G. 2009. Recent insights into cnidarian phylogeny. *Smithson. Contrib. Mar. Sci*. **38:** 139–149.

Collins, A. G., B. Bentlage, A. Lindner, D. Lindsay, S. H. D. Haddock, G. Jarms, J. L. Norenburg, T. Jankowski, and P. Cartwright. 2008. Phylogenetics of Trachylina (Cnidaria: Hydrozoa) with new insights on the evolution of some problematical taxa. *J. Mar. Biol. Assoc. UK* **88:** 1673–1685.

Costello, J. H., S. P. Colin, and J. O. Dabiri. 2008. Medusan morphospace: phylogenetic constraints, biomechanical solutions and ecological consequences. *Invertebr. Biol.* **127:** 265–290.

Dabiri, J. O., S. P. Colin, J. H. Costello, and M. Gharib. 2005. Flow patterns generated by oblate medusan jellyfish: field measurements and laboratory analysis. *J. Exp. Biol.* **208:** 1257–1265.

Dabiri, J. O., S. P. Colin, and J. H. Costello. 2006. Fast-swimming jellyfish exploit velar kinematics to achieve optimal vortex formation. *J. Exp. Biol.* **209:** 2025–2033.

Dabiri, J. O., S. P. Colin, and J. H. Costello. 2007. Morphological diversity of medusan lineages constrained by animal-fluid interactions. *J. Exp. Biol.* **210:** 1868–1873.

Dabiri, J. O., S. P. Colin, K. Katija, and J. H. Costello. 2010. A wake-based correlate of swimming performance and foraging behavior in seven co-occurring jellyfish species. *J. Exp. Biol*. **213:** 1217–1225.

Daniel, T. L. 1983. Mechanics and energetics of medusan jet propulsion. *Can. J. Zool*. **61:** 1406–1420.

Daniel, T. L. 1985. Cost of locomotion: unsteady medusan swimming. *J. Exp. Biol.* **119:** 149–164.

Feitl, K. E., A. F. Millett, S. P. Colin, J. O. Dabiri, and J. H. Costello. 2009. Functional morphology and fluid interactions during early development of the scyphomedusa *Aurelia aurita*. *Biol. Bull*. **217:** 283–291.

Gladfelter, W. G. 1973. A comparative analysis of the locomotory systems of medusoid Cnidaria. *Helgol. Wiss. Meeresunters.* **25:** 228–272.

Higgins, J. E. III, M. D. Ford, and J. H. Costello. 2008. Transitions in morphology, nematocyst distribution, fluid motions, and prey capture during development of the scyphomedusa *Cyanea capillata*. *Biol. Bull*. **214:** 29–41.

Kiørboe, T. 2010. How zooplankton feed: mechanisms, traits and trade-offs. *Biol. Rev*. doi: 10.1111/j.1469-185X.2010.00148.x

Nawroth, J. C., K. E. Feitl, S. P. Colin, J. H. Costello, and J. O. Dabiri. 2010. Phenotypic plasticity in juvenile jellyfish medusae facilitates effective animal-fluid interaction. *Biol. Lett.* **6:** 389–393.

Sahin, M., K. Mohseni, and S. P. Colin. 2009. The numerical comparison of flow patterns and propulsive performances for the hydromedusae *Sarsia tubulosa* and *Aequorea victoria*. *J. Exp. Biol.* **212:** 2656–2667.

Vogel, S. 1994. *Life in Moving Fluids.* Princeton University Press, Princeton.

Weston, J., S. P. Colin, J. H. Costello, and E. Abbott. 2009. Changing form and function during development in rowing hydromedusae. *Mar. Ecol. Prog. Ser.* **374:** 127–134.

Widmer, C. L. 2004. The hydroid and early medusa stages of *Mitrocoma cellularia* (Hydrozoa, Mitrocomidae). *Mar. Biol.* **145:** 315–321.

Williams, T. A. 1994. A model of rowing propulsion and the ontongeny of locomotion in *Artemia* larvae. *Biol. Bull*. **187:** 164–173.